A Ternary Inhibitor for X80 Steel Corrosion in Phosphoric Acid Solution

Yanhua Zhu[1], Liqiang Zhao[1,*], Pingli Liu[1], Jia Zhuang[2], Ming Yang[1]

[1] State Key Laboratory of Oil & Gas Reservoir Geology and Exploitation Engineering, Southwest Petroleum University, Chengdu, China, 610500
[2] School of Materials Science and Engineering, Southwest Petroleum University, Chengdu, China, 610500
[*]E-mail: zyhswpu@163.com

A ternary corrosion inhibitor ($C_{14}H_7NaO_7S$-Mo-Ce) was prepared with alizarin red, sodium molybdate and cerium nitrate, its corrosion inhibition performance for X80 steel in phosphoric acid solution was investigated by chemical and electrochemical methods. Results showed that the inhibitor made up by 1.0g/L alizarin red, 1.0g/L cerium nitrate and 1.0g/L sodium molybdate produced strong synergistic effect, and the inhibition efficiency can reach 99.65%. SEM test showed that the ternary inhibitor formed a compact and complete membrance and effectively prevented the corrosive ions to contact with steel surface. The polarization curve showed that the ternary inhibitor is an anodic corrosion inhibitor. The excellent anti-corrosion efficiency of this ternary inhibitor is attributed to generate binary system of two different substances and successively adsorb on steel surface to produce synergic film.

Keywords: ternary corrosion inhibitor, alizarin red, phosphoric acid, X80 steel, synergy

1. INTRODUCTION

Phosphoric acid is used to derust and degrease on metal surface in certain circumstances. Phosphoric acid is a kind of moderate inorganic acid which can cause corrosion damage of metal materials with different degrees. Since phosphating technology becomes more and more mature with the rapid development of industrial technology, it is considered to be of great research significance to use inhibitor for corrosion protection of metal materials in phosphating medium.

Due to the characteristics of high efficiency and stability, sodium molybdate, as the best alternative to chromate corrosion inhibitor, has been widely applied in many neutral or nearly neutral environments [1-5]. It is a mature inorganic corrosion inhibitor used in circulating cooling water

system [6-8]. However, the reports of sodium molybdate used as corrosion inhibitor for steel in phosphoric acid solution are few. Rare earth salts have better corrosion inhibition effect in neutral solution, but poor inhibition effect in acid solution [9-13]. Alizarin red (3, 4-dihydroxy-9, 10-dioxo-2-anthracenesulfonic acid sodium salt) is a kind of anthraquinone dye with high water solubility, stability and wide application [14-17]. The alizarin red has good anti-corrosion ability due to the characteristics of its molecular structure: the lone pair electrons contained by O atoms of oxo group (=O), hydroxyl (-OH) and sulfonic group ($-SO_3$) on the benzene ring [18-21]. This research attempted to use it as a component to prepare ternary corrosion inhibitor for X80 steel in phosphoric solution with sodium molybdate and cerium nitrate.

2. EXPERIMENTAL

2.1. Materials

All of the cerium nitrate, sodium molybdate, alizarin red, phosphoric acid, ethanol and acetone were obtained from Chengdu Kelon Chemical Reagent Company of China, and of analytical reagent grade. The X80 steel specimens (50mm×10mm×3mm) used in this work were investigated in the as-received condition. Its chemical composition is shown in Tab.1. The $0.1mol \cdot L^{-1}$ H_3PO_4 solution was prepared by diluting the saturated H_3PO_4 with distilled water.

Table 1. Chemical composition of X80 steel (wt%) used in this work

Alloy	C	Si	Mn	P	S	Nb	V	Ti	Cr	Cu	B	Fe
wt%	0.065	0.24	1.58	0.011	0.0028	0.057	0.005	0.024	0.022	0.01	0.0006	Bal.

2.2. Instruments

HH-2K constant temperature water-bath (±0.1°C, Yuhua Instrument Company, Gongyi, China); ZF-9 electronic analytical balance (±0.1mg, Shanghai Tetragonal Electronic Instrument Factory, China); CHI600 Electrochemical workstation (Chenhua Instrument Company, Shanghai, China); Scanning electron microscopy (SEM, JSM-7500F produced by JEOL, Japan); X-ray photoelectron spectrometer (AXIS ULTRA DLD produced by Kratos, England).

2.3. Experimental methods

2.3.1. Preparation of the ternary inhibitor

Cerium nitrate, sodium molybdate and alizarin red in different proportion were first mixed and then dissolved in water, the aqueous solution was the target corrosion inhibitor — a ternary inhibitor $C_{14}H_7NaO_7S-Na_2MoO_4-Ce(NO_3)_3$ which was abbreviated as $C_{14}H_7NaO_7S$-Mo-Ce.

2.3.2. Weight-loss method

The fresh X80 steel was washed with acetone, ethyl alcohol, dried in desiccators and then weighed accurately. The weight loss study was carried out by immersing X80 steel in $0.1 mol \cdot L^{-1}$ H_3PO_4 solution for different times at different temperatures with or without different inhibitors. The steel was hanged in $0.1 mol \cdot L^{-1}$ H_3PO_4 solution, and the temperature was controlled by HH-2K constant temperature water-bath. Then, the steel was taken out, washed with distilled water, acetone and anhydrous ethanol, dried in desiccators and reweighed. The corrosion rate (C_R) was calculated using equation (1):

$$C_R = \frac{10^6 \Delta m}{St} \qquad (1)$$

where C_R ($g \cdot m^{-2} \cdot h^{-1}$) is the corrosion rate of each steel specimen, S (mm^2) is the surface area of steel coupon, t (h) is the time of corrosion reaction and Δm (g) is the weight loss of the steel specimen. The corrosion inhibition efficiency (IE) of corrosion inhibitor was calculated using equation (2):

$$IE = \frac{C_R - C_{Ri}}{C_R} \times 100\% \qquad (2)$$

where C_R ($g \cdot m^{-2} \cdot h^{-1}$) and C_{Ri} ($g \cdot m^{-2} \cdot h^{-1}$) is the average corrosion rate in the uninhibited and inhibited solution, respectively [22].

2.3.3. Electrochemical measurements

Potentiodynamic polarization and electrochemical impedance spectroscopy (EIS) are two techniques which were used to study the corrosion behavior of X80 mild steel in $0.1 mol \cdot L^{-1}$ H_3PO_4 solution with and without inhibitor. All electrochemical experiments were performed at 30°C in an electrochemical cell with three electrodes connected to electrochemical workstation. In which, the standard calomel electrode (SCE) was used as reference electrode, platinum electrode was used as an auxiliary electrode and X80 mild steel of $1 cm^2$ (10mm×10mm) was the working electrode. All potentials were measured versus SCE. All electrochemical experiments were measured after reaching a steady open circuit potential.

Potentiodynamic polarization curves were obtained by changing the electrode potential automatically from -300 to +300mV versus E_{oc} at a scan rate of $0.1 mV \cdot s^{-1}$. The inhibition efficiency (IE_p) was calculated using equation (3):

$$IE_P = \frac{I_{corr} - I'_{corr}}{I_{corr}} \times 100\% \qquad (3)$$

where I_{corr} ($mA \cdot cm^{-2}$) and I'_{corr} ($mA \cdot cm^{-2}$) is uninhibited and inhibited corrosion current density, respectively.

Electrochemical impedance measurements were carried out using AC signals of amplitude 5mV peak to peak at the open-circuit potential (E_{oc}) in the frequency range from $10^5 Hz$ to $10^{-2} Hz$. The inhibition efficiency (IE_E) was calculated using equation (4):

$$IE_E = \frac{R'_p - R_p}{R'_p} \times 100\% \qquad (4)$$

where R_p ($\Omega \cdot cm^2$) and R'_p ($\Omega \cdot cm^2$) is the charge transfer resistance value in the absence and presence of inhibitor, respectively [22].

2.3.4. Surface analysis of X80 steel

The microstructures of X80 steel surface after immersing in 0.1mol·L^{-1} H$_3$PO$_4$ solution with and without different inhibitors were obtained using a scanning electron microscope. The elemental composition of corrosion products on X80 steel surface were obtained using XPS analysis. The microstructure and elemental composition analysis were used to study the corrosion mechanism of X80 steel in 0.1mol·L^{-1} H$_3$PO$_4$ solution and anti-corrosion mechanism of corrosion inhibitor.

3. RESULTS AND DISCUSSION

3.1. Inhibition efficiency of different inhibitors

To compare the inhibition effect of ternary inhibitor with that of sole substances, the inhibition efficiencies of single alizarin red, sodium molybdate and cerium nitrate with different concentrations were calculated by weight loss method after immersing X80 steel samples into 0.1mol·L^{-1} H$_3$PO$_4$ solution for 72h at 30°C.
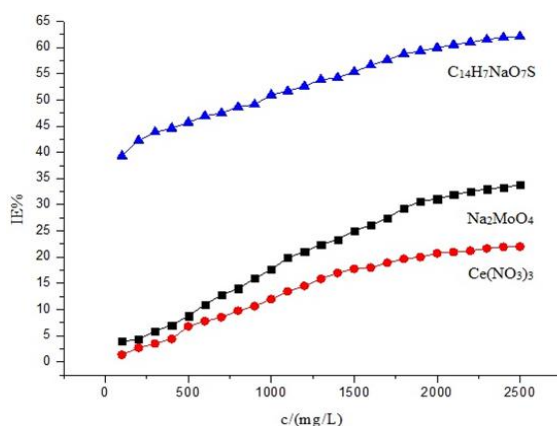
Figure 1. Inhibition efficiency for X80 steel in 0.1mol·L^{-1} H$_3$PO$_4$ solution of different corrosion inhibitor with different concentrations from weight loss method at 30°C for 72h

As shown in Fig.1, the efficiency of Na$_2$MoO$_4$ has a very small increase after the concentration reaches 2.0g/L and the efficiency is less than 35% in the studied concentration range. The authors speculated the inhibition ability of Na$_2$MoO$_4$ in phosphoric acid solution is attributed to that Na$_2$MoO$_4$ generated phosphorus molybdenum blue compounds according to the following reaction [23]:

$$12MoO_4^{2-} + HPO_4^{2-} + 23H^+ = \left[P\left(Mo_{12}O_{40}\right)\right]^{3-} + 12H_2O \qquad (5)$$
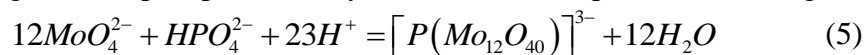
which reduced the hydrogen ion concentration in solution and then inhibited the cathodic dissolving reaction process. In addition, part of the generated phosphorus molybdenum blue acted with Fe^{2+} generated by loss of electronic and then adsorbed on steel surface to prevent the directly contact between steel surface and acid solution [23].

Since the steel surface is positively charged in acid solution, there is strong electrostatic repulsion with Ce^{3+} [24]; However, it is known that Ce^{3+} can't generate insoluble oxide or hydroxide to form a protective film on the steel surface in acid solution according to E-pH program of Ce-H_2O [25]. As shown in Fig.1, $Ce(NO_3)_3$ can only provide a weak inhibition capability, accordingly, $Ce(NO_3)_3$ can't be used as a corrosion inhibitor for X80 steel in H_3PO_4 solution alone.

Fig.1 also shows that the inhibition efficiency of $C_{14}H_7NaO_7S$ increased with increasing concentration and reached 60% when its concentration was 2.0g/L, namely that $C_{14}H_7NaO_7S$ has moderate protection effect for X80 steel in $0.1mol \cdot L^{-1}$ H_3PO_4 solution. The coverage of $C_{14}H_7NaO_7S$ increased with increasing concentration which consistent with the experimental phenomena. The higher inhibitive performance of $C_{14}H_7NaO_7S$ suggests a higher bonding of this triazole to the surface, which possess higher number of lone pairs from heteroatoms and π-orbitals [19].

The results shown in Fig.1 indicated that all of the three substances have poor anticorrosive ability when used alone even with high concentration. This is one of the main reasons which limit their wide application as green inhibitors in engineering. Based on these results, the writer attempted to prepare a ternary inhibitor with these three substances to obtain better inhibition efficiency with less concentration. The results will be discussed in next passages.

3.2. Inhibition effect of the ternary inhibitor

The corrosion inhibition efficiencies of inhibitors made up by 1.0g/L $C_{14}H_7NaO_7S$ and different concentrations of Na_2MoO_4 and $Ce(NO_3)_3$ were evaluated by weight loss method to research the synergy effect between different inhibitors. As shown in Fig.2, the inhibition efficiency of $C_{14}H_7NaO_7S$-Na_2MoO_4 binary inhibitor increased with increasing concentration of Na_2MoO_4, but almost similar to the simple sum of inhibition efficiencies caused by the two kinds of inhibitors, which indicated that there is no synergy effect between $C_{14}H_7NaO_7S$ and Na_2MoO_4. Identically, there is no synergy effect between $C_{14}H_7NaO_7S$ and $Ce(NO_3)_3$, too.

Fig.2 also shows that the inhibition efficiency of $C_{14}H_7NaO_7S$-Mo-Ce ternary inhibitor is much higher than the simple sum of the inhibition efficiencies caused by three kinds of inhibitors, which indicated that there is obvious synergy effect in this system.
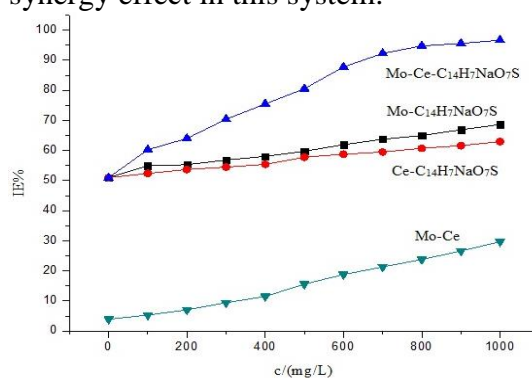
Figure 2. Inhibition efficiency for X80 steel in $0.1mol \cdot L^{-1}$ H_3PO_4 solution of different corrosion inhibitor with different concentrations from weight loss method at 30°C for 72h

3.3. Electrochemical mechanism of the ternary inhibitor

The polarization curves of X80 steel in $0.1\,mol\cdot L^{-1}$ H_3PO_4 solution with and without different inhibitors are shown in Fig.3(a). Some of the authors proposed the following mechanism for the corrosion of iron and steel in acid solution [26-28]:

$$Fe + A^{n-} \rightarrow \left(FeA^{n-}\right)_{ads} \qquad (6)$$

$$\left(FeA^{n-}\right)_{ads} \rightarrow \left(FeA^{n+}\right)_{ads} + ne^{-} \qquad (7)$$

$$\left(FeA^{n+}\right)_{ads} \rightarrow \left(Fe^{2+}\right)_{ads} + A^{n-} \qquad (8)$$
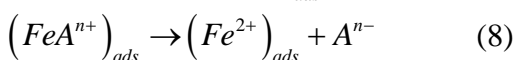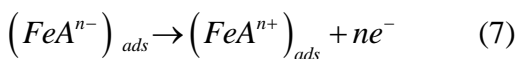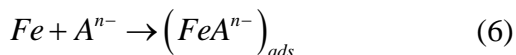
The cathodic hydrogen evolution:

$$Fe + H^{+} \rightarrow \left(FeH^{+}\right)_{ads} \qquad (9)$$

$$\left(FeH^{+}\right)_{ads} + ne^{-} \rightarrow \left(FeH\right)_{ads} \qquad (10)$$

$$\left(FeH^{+}\right)_{ads} + H^{+} + ne^{-} \rightarrow Fe + H_2 \qquad (11)$$

| (a) Polarization curves | (b) Impedance spectrums |
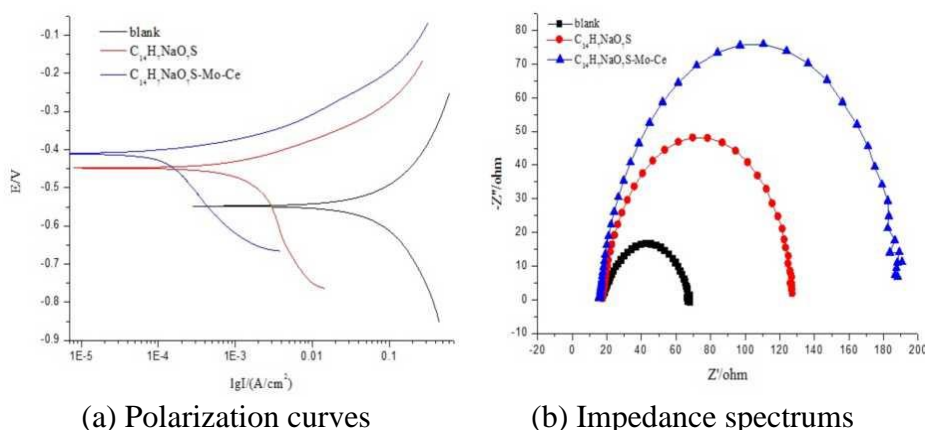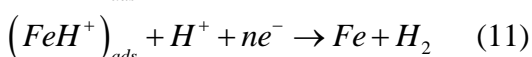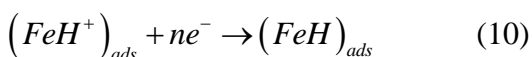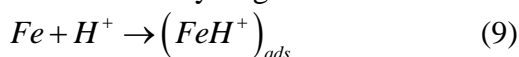
Figure 3. Electrochemical properties of X80 steel in $0.1\,mol\cdot L^{-1}$ H_3PO_4 solution with and without different inhibitors at 30 ℃

Table 2. Electrochemical parameters of X80 steel in $0.1\,mol\cdot L^{-1}$ H_3PO_4 solution with and without different inhibitors obtained by polarization curves at 30 ℃

inhibitor	E_{corr}(mV)	b_a(mV/dec)	$-b_c$(mV/dec)	I_{corr}(mA/cm^2)	IE%
blank	-547	157	108	198.78	—
$C_{14}H_7NaO_7S$	-467	147	122	100.07	49.49
$C_{14}H_7NaO_7S$-Mo-Ce	-390	147	127	9.25	94.95

According to the polarization curves shown in Fig.3(a) and the parameters in Tab.2, the corrosion potential (E_{corr}) of X80 steel obviously moved to positive direction in solution with inhibitor. According to the literatures [29,30], it has been reported that if the displacement in E_{corr} in the presence of inhibitor is more than 85 mV with respect to E_{corr} of the blank, the inhibitor can be recognized as cathodic or anodic type. On the contrary, if the displacement in E_{corr} is less than 85 mV,

the inhibitor can be classified as a mixed type. In this study, the parameters in Tab.2 can demonstrate that the ternary inhibitor is anodic inhibitor that mainly suppresses the anode corrosion process of steel and then decreases the corrosion rate.

The impedance spectrums of X80 steel in $0.1mol·L^{-1}$ H_3PO_4 solution with and without different inhibitors are shown in Fig.3(b). It can be seen that these impedance loops are not perfect semicircles, which can be termed as frequency dispersion effect as a result of the roughness and inhomogeneity of the steel electrode surface [31]. All the impedance spectra displayed in Fig.3(b) reveal a single depressed capacitive semicircle across the studied frequency range, which denotes that the dissolution process is related to the charge transfer process [32]. This inductive arc is generally attributed to anodic adsorbed intermediates controlling the anodic process which is highly agreement with the results of polarization curves.

Table 3. Electrochemical parameters of X80 steel in $0.1mol·L^{-1}$ H_3PO_4 solution with and without different inhibitors obtained by impedance spectrums at 30℃

inhibitor	$R_{ct}(\Omega·cm^2)$	$f_{max}(Hz)$	$C_{dl}(\mu F·cm^{-2})$	*IE*%
blank	55	17.79	157.0	—
$C_{14}H_7NaO_7S$	103	46.25	33.4	46.60
$C_{14}H_7NaO_7S$-Mo-Ce	197	73.34	11.2	72.08

According to the parameters in Tab.3, the steel in solution with ternary inhibitor has the biggest charge transfer resistance and smallest electric double layer capacitor. The larger charge transfer resistance indicated that more inhibitor molecule adsorb on the steel surface and form a protective film on the steel/solution interface [33]. Meanwhile, the smaller value of electric double layer capacitor may be caused by a reduction in local dieletric constant and/or by an increase in the thickness of the electrical double layer [34]. These results indicated that the ternary inhibitor molecules acted by adsorption on the steel/solution interface and formed a layer which can effectively prevent the directly contact between steel surface and corrosive medium, so as to decrease the corrosion rate of X80 steel [35].

3.4. Microstructure of corrosion inhibition films

The inhibition of active dissolution of the steel is due to the adsorption of the inhibitors on the steel surface forming a protective film [36]. The microstructures of protective films on steel surface formed by different inhibitors are shown in Fig.4.

(a) $C_{14}H_7NaO_7S$

(b) $C_{14}H_7NaO_7S$ -Na_2MoO_4

(c) $C_{14}H_7NaO_7S$-$Ce(NO_3)_3$

(d) $C_{14}H_7NaO_7S$ -Na_2MoO_4-$Ce(NO_3)_3$
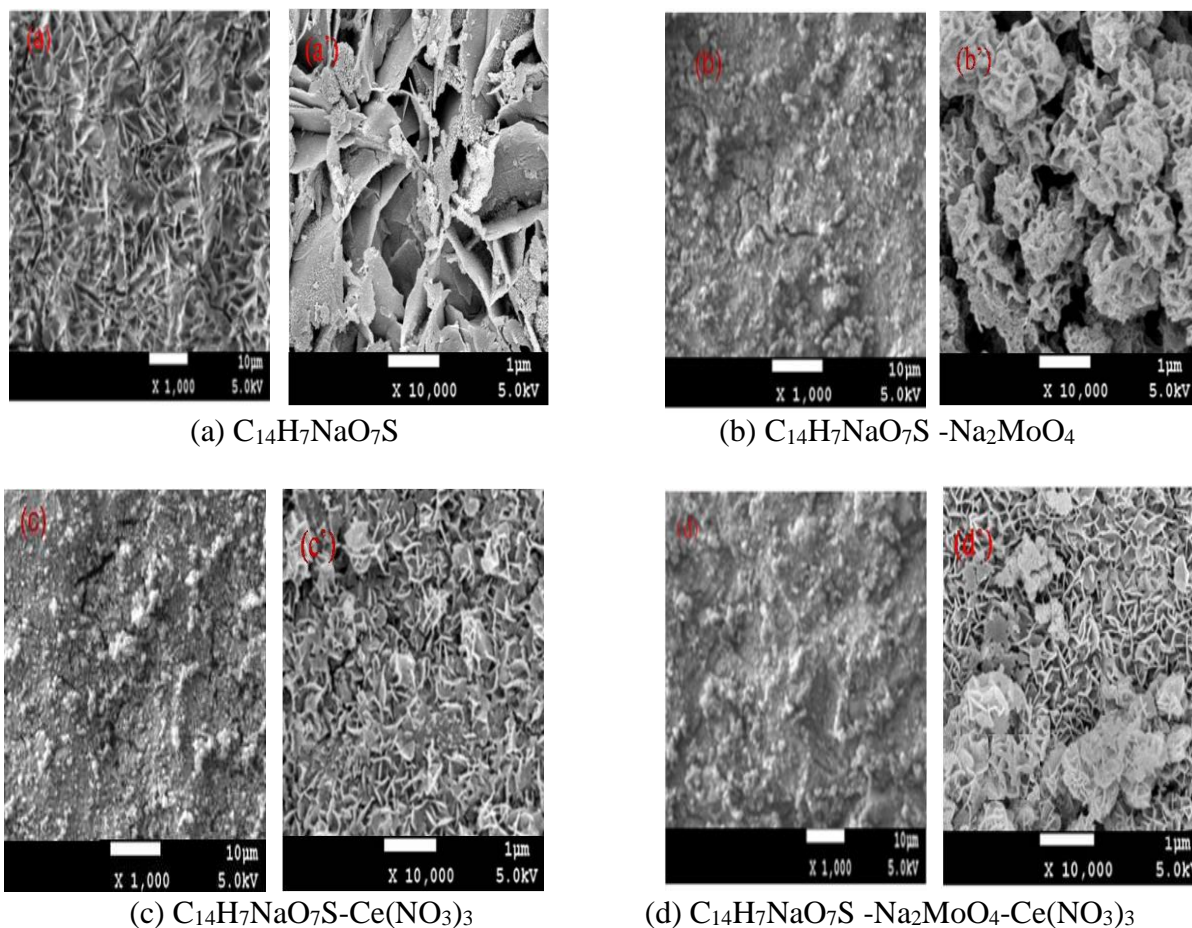
Figure 4. Microstructures of protective films on X80 steel surface formed by different inhibitors after immersion for 72h at 30℃

Fig.4 shows that a dense and integrated protective film was formed on steel surface in solution with $C_{14}H_7NaO_7S$-Mo-Ce ternary inhibitor, this protective film has the ability to resist the damage caused by effect of local stress and always be complete and with high integrity, therefore the corrosion inhibition effect of this ternary inhibitor is excellent. Simultaneously, it can be seen that the microstructure of this integrated film preserved the microstructures of protection films formed by both $C_{14}H_7NaO_7S$-Na_2MoO_4 and $C_{14}H_7NaO_7S$-$Ce(NO_3)_3$ which indicated that the defect of low density caused by different orientations was remedied in the accumulation process of two kinds of structures.

3.5. XPS test of protective film formed by ternary inhibitor

Fig.5 shows the full scan XPS spectra of the surface protective film formed by the ternary inhibitor and indicates that both of the major elements (Mo, O, Na, Ce, C, N) of the inhibitors and the major elements (P, O) of corrosion solution are involved in film. That is to say the corrosive medium is in contact with the film rather than the surface of steel.
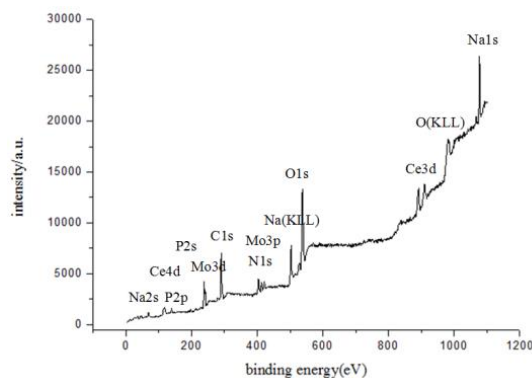
Figure 5. XPS spectra of protective film on steel surface formed by the ternary inhibitor after immersion for 72h at 30℃

3.6. Inhibition mechanism of ternary inhibitor

The mechanism of synergistic effect between various corrosion inhibitors is complex and there is no mature theory to explain this experimental phenomenon. So this paper only speculated the mechanism of synergistic effect of this system.

The results obtained from weight loss method indicated that there is no synergy effect between $C_{14}H_7NaO_7S$ and Na_2MoO_4, $C_{14}H_7NaO_7S$ and $Ce(NO_3)_3$; but obvious synergy effect between $C_{14}H_7NaO_7S$, Na_2MoO_4 and $Ce(NO_3)_3$.

When the three substances of $NaC_{14}H_7O_7S$, Na_2MoO_4 and $Ce(NO_3)_3$ are mixed together, the chelating reaction between Ce^{3+} ions and $C_{14}H_7O_7S^-$ ions for generating $[Ce^{3+}(C_{14}H_7O_7S^-)_3]$ chelate will give preference to happen due to the strong coordination ability of metals and adsorb on steel surface with vertical lamellar morphology structure [37,38]. Then the $C_{14}H_7O_7S^-$ ions react with MoO_4^{2-} ions to form the macrocyclic complex with cotton morphology [39,40], these particles adsorb on the surface of vertical lamellar film formed by Ce^{3+} ions and $C_{14}H_7O_7S^-$ ions shown in Fig.4. Moreover, the particles with cotton morphology mainly adsorb on the defects or cracks of the film with vertical lamellar morphology, act as a filling bridging role. This synergy improves the quality of the membrane and then increases the anti-corrosion efficiency from 61.2% (or 62.3%) to 99.65% significantly. It indicates that the reason for the ternary inhibitor to improve the anti-corrosion efficiency is to generate two kinds of binary system, and successively adsorb on the metal surface to produce synergic film. This kind of synergy is a kind of physical complementary synergy, and the adsorption between two binary substances is the physical adsorption of electrostatic action.

4. CONCLUSION

(1)Alizarin red can be used as a corrosion inhibitor on account of characteristics of its molecular structure and can provide moderate inhibition effect on X80 steel in $0.1mol·L^{-1}$ H_3PO_4 solution when used alone.

(2)All of binary system formed by these three materials cannot show excellent corrosion inhibition effect, there is no obvious synergistic effect between every two combinations; the ternary corrosion inhibitor system has excellent inhibition efficiency which can reach 99.65% was attributed to that there is obvious synergistic effect when the three materials were used at the same time.

(3)The reason of the ternary inhibitor to improve the anti-corrosion efficiency is to generate two different binary system and successively adsorb on the metal surface to produce synergic film.

References

1. W.B. Ran, F.Y. Ma and J.M. Liu, *Contemp. Chem. Ind.,* 39 (2010) 501.
2. H.L. Wang and J.S. Zheng, *Corros. Sci. Prot. Techn.,* 14 (2002) 275.
3. Y.L. Rui, M.X. Lu, Y.H. Liang and Y.L. Wei, *Corros. Prot.,* 28 (2007) 61.
4. J.J. Fang and B. Xu, *Shandong Chem. Ind.,* 37 (2008) 17.
5. Y.Q. Wang, G. Kong, C.S. Che and B. Zhang, *Constr. Build. Mater.,* 162 (2018) 383.
6. Y. Zhou, Y. Zuo and B. Lin, *Mater. Chem. Phys.,* 192 (2017) 86.
7. A. Keyvani, M. Yeganeh and H. Rezaeyan, *Prog. Nat. Sci.-Mater.,* 2 (2017) 261.
8. X.J. Gong, Y.C. Li, K.R. Peng and X.J. Xie, *Corros. Sci. Prot. Techn.,* 13 (2001) 208.
9. A.E. Somers, B.R.W. Hinton, C. Bruin-Dickason, G.B. Deacon and M. Forsyth, *Corros. Sci.,* 139 (2018) 430.
10. C.N.D. Bruin-Dickason, G.B. Deacon, C.M. Forsyth, S. Hanf, O.B. Heilmann, B.R.W. Hinton, P.C. Junk, A.E. Somers, Y.Q. Tan and D.R. Turn, *Aust. J. Chem.,* 70 (2016) 478.
11. B. Volariä and I. Miloå¡Ev, *Brit. Corros. J.,* 52 (2017) 201.
12. B. Davo and J.J. Damborenea, *Electrochim. Acta,* 49 (2004) 4957.
13. G.X.Chen, J.Q.Cao and C.S.Wu, *Mater. Prot.,* 28 (1995) 1.
14. D. Song, X.G. Feng, M.R. Sun, X.X. Ma and G.Z. Tang, *J. Rare Earth.,* 30 (2012) 383.
15. X.H. Li, S.D. Deng, H. Fu, G.N. Mu and N. Zhao, *Appl. Surf. Sci.,* 254 (2008) 5574.
16. J.M. Gao, *Corros. Prot.,* 27 (2006) 151.
17. R.F. Yunus, Y. M. Zheng, K.G.N Nanayakkara and J.P. Chen, *Ind. Eng. Chem. Res.,* 48 (2009) 7466.
18. B. Zheng, H.Z. Ma and B. Wang, *J. Shaanxi Norm. Univ.-Nat. Sci.,* 41 (2013) 55.
19. D.B. Hmamou, R. Salghi, A. Zarrouk, H. Zarrok, B. Hammouti, S.S. Al-Deyab, M. Bouachrine, A. Chakir and M. Zougagh, *Int. J. Electrochem. Sci.,* 7 (2012) 5716.
20. H. Zarrok, R. Salghi, A. Zarrouk, B. Hammouti, H. Oudda, Lh. Bazzi, L. Bammou and S. S. Al- Deyab, *Der Pharma Chemica.,* 4 (2012) 407.
21. E.E. Ebenso, H. Alemu, S.A. Umoren and I.B. Obot, *Int. J. Electrochem. Sci.,* 4 (2008) 1325.
22. L.Q.Zhao, Y.H.Zhu, P.L.Liu, J.Zhang and Y.G.Liu, *Anti-Corros. Method. M*., 64 (2017) 633.
23. Wuhan university and Jilin university, *Inorganic Chemistry, Advanced Education press,*(1994).
24. D.P. Schweinsberg and V. Ashworth, *Corros. Sci.,* 28 (1988) 539.
25. B. Wang, Q.Y. Liu, X.D. Wang, S.J. Jia, J.Lu and H. Dong, *J. Chin. Soc. Corros. Prot.,* 27(2007) 151.
26. M.S. Morad and A. M. K. El-Dean, *Corros. Sci.* 48 (2006) 3398.
27. K. Tebbji, B. Hammouti, H. Oudda, A. Ramdani and M. Benkadour, *Appl. Surf. Sci.* 252 (2005) 1378.
28. A. Yurt, A. Balaban, S. U. Kandemir, G. Bereket and B. Erk, *Mater. Chem. Phys.* 85 (2004) 420.
29. A.A.F. Sabirneeza and S. Subhashini, *Int. J Ind. Chem.*, 5 (2014) 111.
30. E.S. Ferreira, C. Giacomelli and F.C. Giacomelli, *Mater. Chem. Phys.,* 83 (2004) 129.
31. A. Anejjar, R. Salghi and A. Zarrouk, *Res. Chem. Intermediat.*, 41(2015) 913.
32. P.K. Ghosh, D.K. Guhasarkar and V.S. *Gupta, Brit. Corros. J.*, 18 (2013) 187.
33. K. Tebbji, B. Hammouti, H. Oudda, A. Ramdani and M. Benkadour, *Appl. Surf. Sci.*, 252 (2005) 1378.
34. Y. Abboud, A. Abourriche, T. Saffaj, M. Berrada and M. Charrouf, *Appl. Surf. Sci*., 252 (2006)

8178.

35. D.A. Lopez, T. Perez, S. N. Simison, *Mater. Design*, 24 (2003) 561.
36. L.D. Paolinelli, T. Perez, S.N. Simison. *Corros. Sci*., 50 (2008) 2456.
37. A.K. Singh and M.A. Quraishi, *Corros. Sci.*, 51 (2009) 2752.
38. M.H. Zhai, X.W. Wei and Q.Q. Zha, *Coordination Chemistry, Anhui People's Press,* (2007).
39. M. Li, Z.G. Liu, J.X. Wu, Y.H. Hu, *Rare Earth Element and Analytical Chemistry*, *Chemical Industry Press,* (2009).
40. J.J. Lin and J. Wang, *Inorganic Chemistry*, *Beijing Chemical Industry Press,* (2006).